# Unfolding Rates of Barstar Determined in Native and Low Denaturant Conditions Indicate the Presence of Intermediates †

**ARTICLE** *in* BIOCHEMISTRY · MARCH 2002

Impact Factor: 3.02 · DOI: 10.1021/bi011494v · Source: PubMed



**2 AUTHORS**, INCLUDING:

Jayant B Udgaonkar
Tata Institute of Fundamental Research
**147** PUBLICATIONS **4,298** CITATIONS

# Unfolding Rates of Barstar Determined in Native and Low Denaturant Conditions Indicate the Presence of Intermediates†

K. Sridevi and Jayant B. Udgaonkar*

*National Centre for Biological Sciences, Tata Institute of Fundamental Research, GKVK Campus, Bangalore, India 560065*

*Received July 17, 2001; Revised Manuscript Received November 5, 2001*

ABSTRACT: The folding and unfolding rates of the small protein, barstar, have been monitored using stopped-flow measurements of intrinsic tryptophan fluorescence at 25 °C, pH 8.5, and have been compared over a wide range of urea and guanidine hydrochloride (GdnHCl) concentrations. When the logarithms of the rates of folding from urea and from GdnHCl unfolded forms are extrapolated linearly with denaturant concentration, the same rate is obtained for folding in zero denaturant. Similar linear extrapolations of rates of unfolding in urea and GdnHCl yield, however, different unfolding rates in zero denaturant, indicating that such linear extrapolations are not valid. It has been difficult, for any protein, to determine unfolding rates under nativelike conditions in direct kinetic experiments. Using a novel strategy of coupling the reactivity of a buried cysteine residue with 5,5′-dithiobis(2-nitrobenzoic acid) (DTNB) to the unfolding reaction of barstar, the global unfolding and refolding rates have now been determined in low denaturant concentrations. The logarithms of unfolding rates obtained at low urea and GdnHCl concentrations show a markedly nonlinear dependence on denaturant concentration and converge to the same unfolding rate in the absence of denaturant. It is shown that the native protein can sample the fully unfolded conformation even in the absence of denaturant. The observed nonlinear dependences of the logarithms of the refolding and unfolding rates observed for both denaturants are shown to be due to the presence of (un)folding intermediates and not due to movements in the position of the transition state with a change in denaturant concentration.

Characterization of the structures and stabilities of the various conformational states that a polypeptide chain can sample is a principal goal of protein folding studies. The stability of a protein, in terms of the free energy change ($\Delta G_U$) that occurs upon unfolding from the native (N) state to the unfolded (U) form, is commonly determined by the analysis of denaturant-induced or thermally induced equilibrium unfolding transitions, where the structural changes occurring during the unfolding transition can be monitored spectroscopically. The observation of a cooperative unfolding transition allows the determination of the stability of the native protein by use of a two-state, N ⇌ U, model, and $\Delta G_U$ obtained in the presence of denaturant is extrapolated linearly with denaturant concentration according to the linear free energy model (*1*) to obtain $\Delta G_U(H_2O)$, the free energy of unfolding in the absence of denaturant. The linear free energy model has been validated strongly by studies utilizing combined analyses of GdnHCl[1]-induced and temperature-induced unfolding transitions (*2*). More recently, validation of the use of the linear free energy model has come from hydrogen exchange (HX) studies (*3*−*5*).

The free energy of activation of a folding or unfolding reaction is also assumed to have a linear dependence on denaturant concentration, because the folding and unfolding rate constants observed for many proteins show exponential dependences on denaturant concentration (*6*−*9*). Thus, the logarithms of the folding and unfolding rates determined in the presence of denaturant are typically extrapolated linearly with denaturant concentration to determine the rates at zero denaturant. For a number of proteins that fold genuinely by a two-state mechanism, there is good agreement between the $\Delta G_U(H_2O)$ values obtained by linear extrapolation of free energy changes in an equilibrium unfolding transition and from the linear extrapolation of the logarithm of the ratio of the unfolding to folding rates obtained from kinetic experiments (*6*−*9*; listed in ref *10*). Other support for the legitimacy of linear extrapolation of the logarithm of a folding or unfolding rate comes from a recent study of the folding of ubiquitin, where the unfolding rates obtained experimentally at low denaturant concentrations using HX have been shown to agree with the rates obtained by linear extrapolation of the rates obtained at high denaturant concentrations by optical spectroscopic methods (*11*).

The agreement of $\Delta G_U(H_2O)$ values obtained from equilibrium and kinetic experiments is an essential criterion for a two-state process, and disagreement between these values is taken as evidence for the presence of intermediates (*12*). The value for $\Delta G_U(H_2O)$ obtained from kinetic experiments may, however, be erroneous if the logarithm of the rate constants varies nonlinearly with denaturant concentration

† This work was funded by the Tata Institute of Fundamental Research, by the Department of Science and Technology, Government of India, and by the Wellcome Trust. J.B.U. is the recipient of a Swarnajayanti Fellowship from the Government of India.

* Corresponding author. E-mail: jayant@ncbs.res.in. Fax: 91-80-3636662.

[1] Abbreviations: DTNB, 5,5′-dithiobis(2-nitrobenzoic acid); GdnHCl, guanidine hydrochloride; HX, hydrogen exchange; SX, thiol exchange; EDTA, ethylenediaminetetraacetic acid; CD, circular dichroism.

10.1021/bi011494v CCC: $22.00 
Published on Web 01/11/2002

(*13*−*16*). Curvature can arise when intermediates are present on the folding or unfolding pathway (*15*, *17*−*21*), due to denaturant-induced changes in the rate-limiting kinetic step (*12*). Alternatively, curvature can result from Hammond behavior (*14*) in which the structure of the transition state changes with denaturant to resemble the least stable state under the experimental conditions (*16*, *22*). The observation of such nonlinear dependence of the logarithm of rates on denaturant concentration for several proteins (*13*−*16*) questions the validity of the linear extrapolations commonly used to determine the unfolding rates in nondenaturing conditions. Even when the logarithms of the unfolding rates show linear denaturant dependences at high denaturant concentrations, the linear extrapolation of log rates obtained in high urea and GdnHCl concentrations may result in different unfolding rates at zero denaturant concentration. For example, the unfolding rate for barnase obtained by linear extrapolation of rates in GdnHCl is 10-fold lower than the rate obtained similarly from urea-induced unfolding (*13*, *23*). Thus, linear extrapolations of unfolding rates determined at high denaturant concentrations can be misleading, and in the absence of experimental data concerning unfolding kinetics at low denaturant concentrations, it is difficult to determine the folding and unfolding pathways accessible to the native protein under nondenaturing conditions. These problems clearly highlight the importance of determining the folding and unfolding rates in the absence of denaturant and at low denaturant concentrations, so as to eliminate the need for extrapolations from data obtained at high denaturant concentrations.

Barstar, a protein extensively used for protein folding studies (*24*−*30*), serves as a model system to understand the denaturant dependence of folding and unfolding rates. The validity of the linear free energy model to obtain $\Delta G_U(H_2O)$ from the $\Delta G_U$ obtained in a GdnHCl-induced unfolding transition on the basis of a two-state model has been verified experimentally for barstar (*2*). Also, the values of $\Delta G_U(H_2O)$ obtained from urea-induced and GdnHCl-induced equilibrium unfolding transitions are identical, further validating the determination of $\Delta G_U(H_2O)$ on the basis of the linear free energy model. This value for $\Delta G_U(H_2O)$ is, however, not correctly predicted from the observed fluorescence-monitored folding and unfolding rates in urea (*24*) or GdnHCl (*26*).

The folding as well as unfolding reactions of barstar appear to be multistate with discrete intermediates populating parallel pathways (*20*, *24*−*30*). The Tyr47−Pro48 bond is in the *cis* conformation in the native state, and upon unfolding, it can exist in both the *cis* ($U_F$ or the fast folding form) and *trans* ($U_S$ or the slow folding form) conformations. Native barstar in high denaturant concentration unfolds to $U_F$ via parallel competing pathways where intermediates have been detected (*20*, *28*−*29*). In the work presented here, the folding rates and unfolding rates for the $N \rightleftharpoons U_F$ transition of barstar have been determined using a thiol reaction strategy similar to native state hydrogen exchange methodology.

Pulsed HX experiments have provided detailed information about folding pathways and intermediates during folding (see ref *5* for review). In a similar manner, the reactivity of the thiol group of cysteine side chains has been used in pulsed thiol−disulfide exchange experiments to study folding and unfolding pathways (*29*, *31*). Native state HX experiments can measure equilibrium stability parameters under native conditions (*32*). When a protein has hydrogens that exchange only from the globally unfolded state, their measured HX rates can be used to compute the free energy of the global unfolding equilibrium under the conditions of the HX measurement. Similarly, the global unfolding rates at equilibrium can be determined by monitoring the reactivity of the thiol of a buried cysteine residue which becomes exposed only upon global unfolding. Barstar has two buried cysteine residues: Cys40 and Cys82. The accessibility of the buried cysteine to thiol-modifying agents such as DTNB is easily monitored (*29*). Since DTNB can react only with an exposed thiol, the observed rate of labeling of a cysteine will depend on the rate of exposure of the buried cysteine side chain. A mutant of barstar, containing a single core tryptophan (Trp53) and a single cysteine (Cys82), was used for the DTNB labeling studies described here. The advantage of using this mutant is that the fluorescence-monitored kinetics can be assigned to changes occurring in the environment of the core tryptophan, and the Cys82 thiol provides a unique buried site for the DTNB reaction.

The protein was equilibrated in different concentrations of denaturant and reacted with DTNB. The rate of the DTNB reaction at every denaturant concentration was monitored for different concentrations of DTNB. The dependence of the observed DTNB reaction rate on the DTNB concentration clearly indicates that a structural transition precedes the labeling reaction and the rates for this transition could be determined from the observed labeling rates. The results indicate that, under native conditions, the protein can unfold to the fully unfolded form, similar to the denaturant-induced unfolded form. The data also reveal that intermediates are populated during the transition of the native state to the unfolded form.

## MATERIALS AND METHODS

*Protein Purification.* The mutant protein W38F/W44F/C40A containing a single tryptophan (Trp53) and a single cysteine (Cys82) was prepared as described earlier (*33*). Protein concentration was determined by absorbance at 280 nm, using $\epsilon_{280} = 10000\ M^{-1}\ cm^{-1}$.

*Buffers and Solutions.* All experiments were done at 25 °C, in buffer containing 100 mM Tris and 0.5 mM EDTA at pH 8.5. Concentrations of stock urea or GdnHCl solutions were determined by refractive index measurements. The concentration of the stock DTNB solution was determined by absorbance at 325 nm, using an $\epsilon_{325} = 17380\ M^{-1}\ cm^{-1}$ (*34*). In all of the experiments, the protein concentration used was 10 $\mu$M, and the DTNB concentration was varied between 0.5 and 8.0 mM.

*Measurement of Unfolding and Refolding Rates for the $N \rightleftharpoons U_F$ Transition by Fluorescence*. The unfolding and refolding experiments in different denaturant concentrations were done in the stopped-flow module, SFM 400, from Biologic, France. The fluorescence changes during the kinetics were monitored at 320 nm upon excitation at 295 nm, using the MOS-250 detection system from Biologic. To obtain the refolding rates of $U_F$, the refolding of the transiently unfolded protein was monitored (*26*). Native barstar was unfolded for 6 s in different urea and GdnHCl

concentrations and then refolded by dilution of denaturant. This short unfolding time does not allow proline isomerization to occur, and $U_S$ is therefore not formed. The folding rates so obtained correspond to the $U_F \rightarrow N$ transition.

*Measurement of Equilibrium Unfolding Transitions*. For equilibrium unfolding measurements, barstar solutions containing different concentrations of denaturant were incubated for ~3 h (incubations ranging from 2 to 24 h gave the same results). Tryptophan fluorescence excited at 295 nm was monitored at 320 nm using a SPEX Fluorolog fluorimeter. Circular dichroism (CD) measurements at 222 nm were made on a Jasco 720 spectropolarimeter.

*Measurement of Cysteine Labeling Rates*. The free thiol group of cysteine reacts with DTNB at alkaline pH, resulting in the attachment of one TNB group to the cysteine, and the release of one $TNB^-$. The rate of reaction can therefore be monitored by measurement of the increase in absorbance at 412 nm due to the release of $TNB^-$. The amount of protein labeled can be determined from the fraction of $TNB^-$ released, using $\epsilon_{412} = 14100\ M^{-1}\ cm^{-1}$ (*34*). Under the experimental conditions used, the entire labeling kinetics were observable, and 100% labeling was obtained at all denaturant and DTNB concentrations. The labeling reactions were carried out by mixing the protein equilibrated in different denaturant concentrations with DTNB in the same denaturant concentration in the SFM 400 module. Thus, the denaturant concentration did not vary at all during the labeling reaction. Labeling kinetics in the native state and in low denaturant concentration were also monitored in a CARY 100 UV−VIS spectrophotometer, where the reactions were initiated manually.

The bimolecular rate constant for the reaction of the cysteine thiol with DTNB depends on the temperature, pH, and ionic strength (*35*). Also, charged residues adjacent in sequence to the cysteine influence the labeling rate (*36*). To determine the bimolecular rate constant for the reaction of DTNB with a fully exposed Cys82, the labeling reaction was also carried out on a pentapeptide corresponding to the sequence flanking Cys82 in barstar (EGCDI). The peptide was purchased from Chiron Technologies, Australia. The DTNB labeling experiments of the peptide were done under the same conditions as the protein in the presence of different denaturant concentrations.

*Data Analysis. (A) Analysis of Fluorescence Monitored Kinetics*. The rates observed for the $N \rightleftharpoons U_F$ reaction monitored by fluorescence vary exponentially with denaturant concentration in the range of denaturant concentration used in these experiments and were fit to the equations:

$$\ln \lambda_f = \ln \lambda_f^{H_2O} - m_{\lambda_f}[\text{denaturant}] \quad (1a)$$

$$\ln \lambda_u = \ln \lambda_u^{H_2O} + m_{\lambda_u}[\text{denaturant}] \quad (1b)$$

where $\lambda_f^{H_2O}$ and $\lambda_u^{H_2O}$ are the values of the rates in the absence of denaturant and $m_{\lambda_f}$ and $m_{\lambda_u}$ represent the dependences of these rates on denaturant concentration.

For a two-state transition, the values of $\lambda_f^{H_2O}$, $\lambda_u^{H_2O}$, $m_{\lambda_f}$, and $m_{\lambda_u}$ determined from the fits can be used to obtain $\Delta G_U$ [$= -RT \ln(\lambda_u/\lambda_f)$] and its denaturant dependence, given by

$$\Delta G_u = \Delta G_u^{H_2O} + m_G[\text{denaturant}] \quad (2)$$

Combining eqs 1 and 2 gives

$$\Delta G_u(H_2O) = -RT \ln \frac{\lambda_u^{H_2O}}{\lambda_f^{H_2O}} \quad (3a)$$

$$m_G = -RT(m_{\lambda_u} + m_{\lambda_f}) \quad (3b)$$

The values for $\Delta G_U(H_2O)$ and $m_G$ obtained by the above analysis of rates can be compared to the same values obtained by a two-state analysis using the linear free energy model (*2*, *37*) of the equilibrium unfolding transition monitored by CD or fluorescence. For barstar, however, the $\Delta G_U(H_2O)$ obtained from a two-state analysis of the equilibrium unfolding transition corresponds to the free energy difference between the native state and an equilibrium mixture of $U_F$ and $U_S$ states. The difference in free energy change for the $N \rightleftharpoons U_F$ reaction and the $N \rightleftharpoons U_F \rightleftharpoons U_S$ reaction ($\Delta\Delta G$) depends on the energy difference between the two unfolded forms differing in the isomerization of one proline bond. The equilibrium constant $K = U_F/U_S$ is 0.47 (*25*); thus, $\Delta\Delta G = -RT \ln(K/1 + K) = 0.7$ kcal/mol. After addition of 0.7 kcal/mol, the value of $\Delta G_U$ obtained from optically monitored equilibrium unfolding transitions was found to be consistent with the free energy change for a group of amide protons obtained by hydrogen exchange (*3*). Thus, the value for $\Delta G_U(H_2O)$ obtained from the two-state analysis of the equilibrium unfolding transition was corrected for the proline-related step by addition of 0.7 kcal/mol, so that it could be compared with the value obtained from extrapolation of rates for the $N \rightleftharpoons U_F$ reaction.

*(B) Analysis of Cysteine Labeling Rates*. The bimolecular rate constant for the reaction of cysteine with DTNB ($k_b$) was determined by obtaining labeling rates at different DTNB concentrations for the peptide (EGCDI). The observed kinetics of release of $TNB^-$ during labeling of the peptide fit to a single-exponential equation, with one apparent rate constant. This apparent rate constant was determined at different DTNB concentrations, and the slope of the rate constant vs DTNB concentration gives the bimolecular rate constant, which was then determined at different denaturant concentrations.

The observed kinetics of release of $TNB^-$ during labeling of the protein fit either to a single exponential or to a biexponential equation, depending on the concentration of denaturant used. When the $TNB^-$ release kinetics fit to a double exponential, then the relative amplitudes corresponding to the two apparent rate constants gave the fraction of molecules reacting with that rate.

The slow labeling rate observed for the native protein, and at low denaturant concentrations, was fit to the thiol−disulfide exchange mechanism:

mechanism 1

$$\text{closed (SH)} \underset{k_{cl}}{\overset{k_{op}}{\rightleftharpoons}} \text{open (SH)} \xrightarrow{k_{ex}} \text{exchanged (STNB)}$$

In this model, exchange-competent [open(SH)] and exchange-incompetent [closed(SH)] conformations interconvert with rate constants $k_{op}$ and $k_{cl}$, respectively. Exchange occurs only from the open conformation with an intrinsic exchange rate constant $k_{ex}$ ($=k_b$[DTNB]). The equation describing exchange

at equilibrium can be obtained by using Cleland's method of net rate constants (*38*), where each rate step is reduced to a net rate constant ($k'$), and the procedure of summing the transit times ($1/k'$) for each step (*39*):

$$k_{ex} = -(k_{op} + k_{cl}) + k_{op}\left(\frac{k_{ex}}{k_{obs}}\right) \quad (4a)$$

Equation 4a can be rearranged to eq 4b, which defines the dependence of the observed slow labeling rates ($k_{obs}$) on DTNB concentration:

$$k_{obs} = \frac{k_{op}k_b[\text{DTNB}]}{k_{op} + k_{cl} + k_b[\text{DTNB}]} \quad (4b)$$

Plots of $k_{obs}$ vs [DTNB] were fit to eq 4b to obtain $k_{op}$ and $k_{cl}$. At each denaturant concentration, the DTNB dependence of the labeling rate was determined from three to four independent experiments. This allowed the errors in the values of $k_{op}$ and $k_{cl}$ to be estimated as the standard deviation from three repetitions at each denaturant concentration.

If the exchange-competent state (open SH) in mechanism 1 corresponds to the globally unfolded state (U), $k_{op}$ and $k_{cl}$ will correspond to the global unfolding and folding rates, respectively, for a two-step opening−closing transition.

If the opening−closing transition is not a two-state process, and an intermediate (I) is present on the pathway from the closed native state (N) to the open unfolded state (U), but exchange occurs only from the U state, according to the mechanism:

mechanism 2

$$\text{N} \underset{k_{-1}}{\overset{k_1}{\rightleftharpoons}} \text{I} \underset{k_{-2}}{\overset{k_2}{\rightleftharpoons}} \text{U} \overset{k_{ex}}{\rightleftharpoons} \text{UTNB}$$

then the observed exchange rate, obtained by the method of net rate constants, is given by

$$k_{ex} = \frac{k_1k_2 + k_1k_{-2} + k_{-1}k_{-2}}{k_{-1} + k_1 + k_2} + \frac{k_1k_2}{k_{-1} + k_1 + k_2}\left(\frac{k_{ex}}{k_{obs}}\right) \quad (5)$$

A comparison of eq 5 with eq 4a indicates that the overall opening rate constant $k_{op}$ for labeling according to mechanism 2 is given by

$$k_{op} = \frac{k_1k_2}{k_{-1} + k_1 + k_2} \quad (6)$$

Assuming a fast preequilibrium between N and I (that is, $k_1$, $k_{-1} > k_2$), the observed unfolding rate constant, $\lambda_u$, which is equal to the overall opening rate constant $k_{op}$, is given by

$$\lambda_u = \frac{K_1k_2}{1 + K_1} \quad (7)$$

where $K_1$ is the equilibrium constant for the N to I transition. Since the global unfolding equilibrium constant, $K_U$ ($=\lambda_u/\lambda_f = k_{op}/k_{cl}$) is, according to mechanism 2, equal to $K_1k_2/k_{-2}$, the observed folding rate $\lambda_f$, which is equal to the overall closing rate $k_{cl}$, is given by

$$\lambda_f = \frac{k_{-2}}{1 + K_1} \quad (8)$$

$K_1$ and $k_2$ can be determined by fitting the unfolding rates to eq 7, and $k_{-2}$ can be determined by fitting the observed folding rates to eq 8.

All of the fitting procedures were carried out using Sigmaplot 5.0. The goodness of the fits of the various equations to the data was estimated by the multiple correlation coefficient ($R$). All of the fits had $R$ values between 0.95 and 0.99, indicating that the equations used were satisfactory.

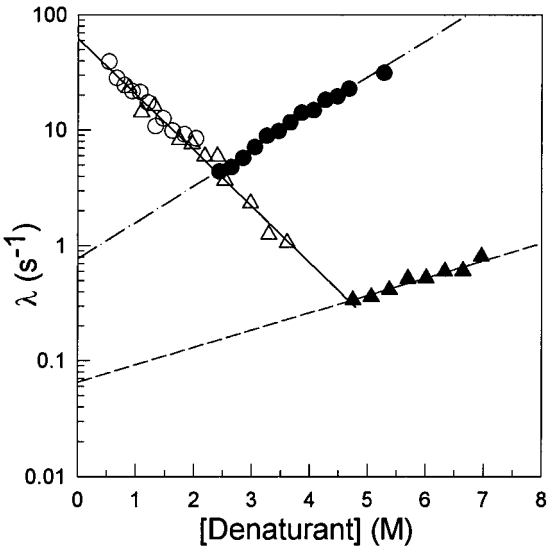


FIGURE 1: Observed folding and unfolding rates for the $N \leftrightarrows U_F$ transition of barstar at 25 °C, pH 8.5. The rates of folding (open symbols) and unfolding (closed symbols) were measured in different concentrations of urea (triangles) and GdnHCl (circles) by monitoring the changes in the intrinsic tryptophan fluorescence at 320 nm upon excitation at 295 nm. The solid line through the refolding data represents the equation $\log \lambda_f = \log(63) - 0.5[\text{denaturant}]$. The dashed lines through the unfolding rates represent $\log \lambda_u = \log(0.06) + 0.15[\text{urea}]$ and $\log \lambda_u = \log(0.78) + 0.31[\text{GdnHCl}]$.

## RESULTS

*Kinetics Monitored by Fluorescence.* The refolding and unfolding kinetics were monitored for the $N \rightleftharpoons U_F$ transition to allow comparison with the rates obtained from the cysteine labeling experiments, because the cysteine is expected to be completely exposed in $U_F$, and the DTNB reaction rate is much faster than the proline isomerization step that leads to the formation of $U_S$. Refolding rates of $U_F$ were measured by transiently unfolding N in urea or GdnHCl, followed by refolding (see Materials and Methods). It can be seen from Figure 1 that the refolding rates are identical in urea and GdnHCl. Also, the refolding rates obtained for this mutant of barstar are similar to those obtained earlier for wt barstar (*24*, *26*). The measured refolding rates fit well to eq 1a.

The fast phase of the unfolding of N corresponds to unfolding to the $U_F$ state. The unfolding rates in urea and GdnHCl have different denaturant dependences and also do not extrapolate to the same $\lambda_u^{H_2O}$ when fit to eq 1b (Figure 1). This clearly indicates that eq 1b describing the linear

dependence of the logarithm of the unfolding rate constant is not appropriate for fitting the data. The incorrectness of the linear extrapolations according to eqs 1a,b is further borne out by the extrapolated rates in water not predicting the value of $\Delta G_U(H_2O)$ and its denaturant dependence obtained from the equilibrium unfolding transition (eqs 3a,b).

The equilibrium unfolding transitions monitored by CD and fluorescence are similar. A two-state analysis of the data gives a value for $\Delta G_U(H_2O)$ of 4.2 ± 0.5 kcal mol$^{-1}$ and for $m_G$ of 1.2 ± 0.1 kcal mol$^{-1}$ M$^{-1}$ in urea and 2.4 ± 0.1 kcal mol$^{-1}$ M$^{-1}$ in GdnHCl (*40*). The value for $\Delta G_U(H_2O)$ for the N ⇌ $U_F$ transition is obtained by adding the energy difference (~0.7 kcal mol$^{-1}$) to correct for the proline-related $U_F$ ⇌ $U_S$ step (see Materials and Methods). Thus, the value for $\Delta G_U(H_2O)$ for unfolding to $U_F$ is 4.9 ± 0.5 kcal mol$^{-1}$. The value for $\Delta G_U(H_2O)$ obtained by extrapolation of unfolding and refolding rates to low denaturant concentrations (~3.9 kcal mol$^{-1}$ from rates in urea, 2.5 kcal mol$^{-1}$ from rates in GdnHCl) does not agree with the value of $\Delta G_U(H_2O)$ obtained from equilibrium measurements. Also, the denaturant dependence of $\Delta G_U(H_2O)$ obtained from the equilibrium unfolding transition in urea and GdnHCl does not match that obtained from the rate dependences (~0.8 kcal mol$^{-1}$ M$^{-1}$ in urea and 1.2 kcal mol$^{-1}$ M$^{-1}$ in GdnHCl). Thus, it is clear that the linear extrapolation of the logarithm of the folding and unfolding rates for the N ⇌ $U_F$ transition of barstar is inadequate.

*Cysteine Labeling Kinetics*. The reaction of a buried thiol group with DTNB can be used to determine the unfolding and refolding rate when the two reactions are coupled. Protein equilibrated in different denaturant concentrations was reacted with DTNB, also at the same denaturant concentration, and the rate of the labeling reaction was monitored by the release of $TNB^-$ (Figure 2). A single, slow labeling rate is observed for the native protein and in low denaturant concentrations (Figure 2a). Biphasic labeling kinetics are observed at intermediate denaturant concentrations, and a single fast labeling rate is seen at high denaturant concentrations (Figure 2b,c).

The fractional amplitude of the fast labeling rate corresponds to the fraction of unfolded protein, as determined from a two-state analysis of the equilibrium unfolding transition monitored by either CD or fluorescence (Figure 3a,b). This indicates that all molecules that are labeled at the fast rate have the same exposure of the cysteine residue as does U. When the labeling reaction is done in increasing DTNB concentrations, the fast labeling rate increases linearly with DTNB concentration (data not shown). The slope of the DTNB dependence gives the bimolecular rate constant for the labeling reaction. Since the bimolecular rate constants could be obtained only in the transition and posttransition regions for the protein where the fast labeling rate is observed, labeling was also done with a pentapeptide corresponding to the sequence flanking Cys82 in barstar over the entire denaturant range in both urea and GdnHCl. The bimolecular rate constants obtained from the fast labeling reaction of the protein and the peptide (Figure 3c,d) agree well. An initial increase in the bimolecular rate constant with GdnHCl concentration below 0.2 M is observed for the peptide (Figure 3d). This is probably due to the increase in the labeling rate with increasing ionic strength as reported earlier for this reaction (*36*). At GdnHCl concentrations

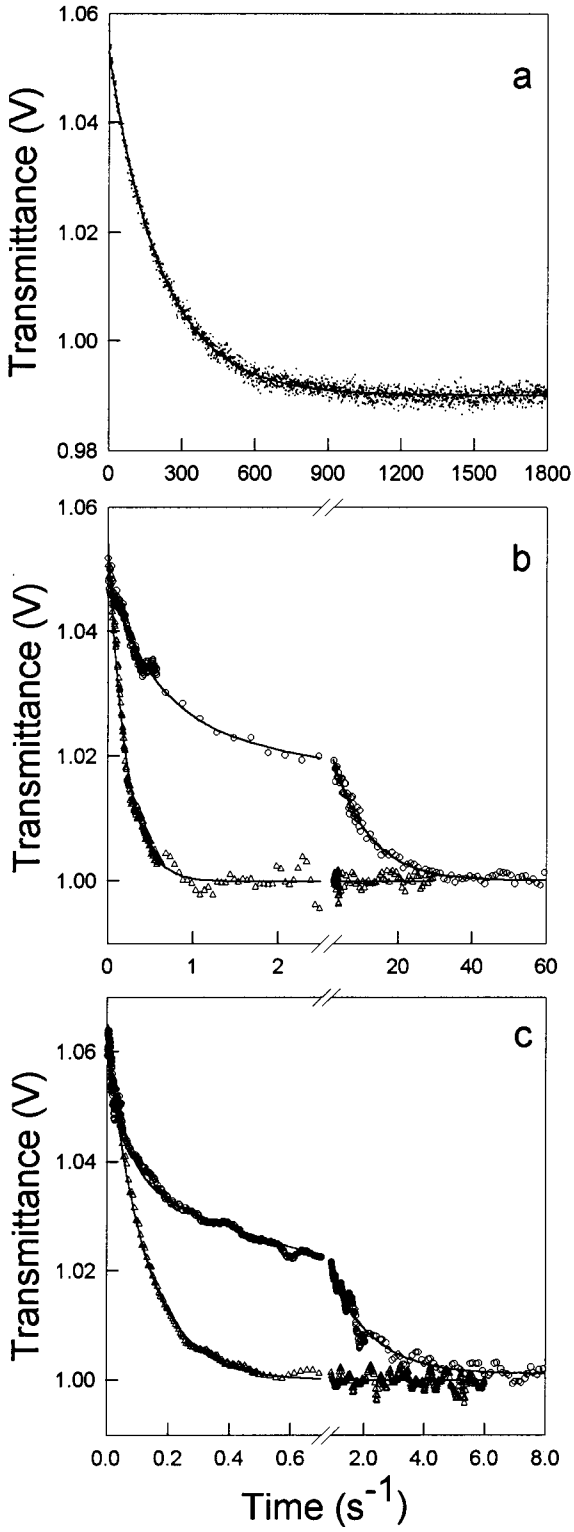


FIGURE 2: Representative data of kinetics of labeling of barstar with DTNB at 25 °C, pH 8.5. Native protein or protein incubated in different denaturant concentrations was reacted with DTNB, and the progress of the reaction was monitored by the change in transmittance at 412 nm due to release of $TNB^-$. (a) Labeling of native protein with DTNB; the solid line is a fit to a single-exponential equation with an apparent rate of 0.0046 s$^{-1}$. (b) Labeling of protein incubated in 3.5 M urea (circles), fit to a biexponential equation with rates of 1.9 and 0.1 s$^{-1}$, and protein in 7 M urea (triangles), fit to a single exponential with a rate of 4.7 s$^{-1}$. (c) Labeling of protein incubated in 1.5 M GdnHCl (circles), fit to a biexponential equation with rates of 16.9 and 0.73 s$^{-1}$, and protein in 4.2 M GdnHCl (triangles), fit to a single-exponential equation with a rate of 8.05 s$^{-1}$.

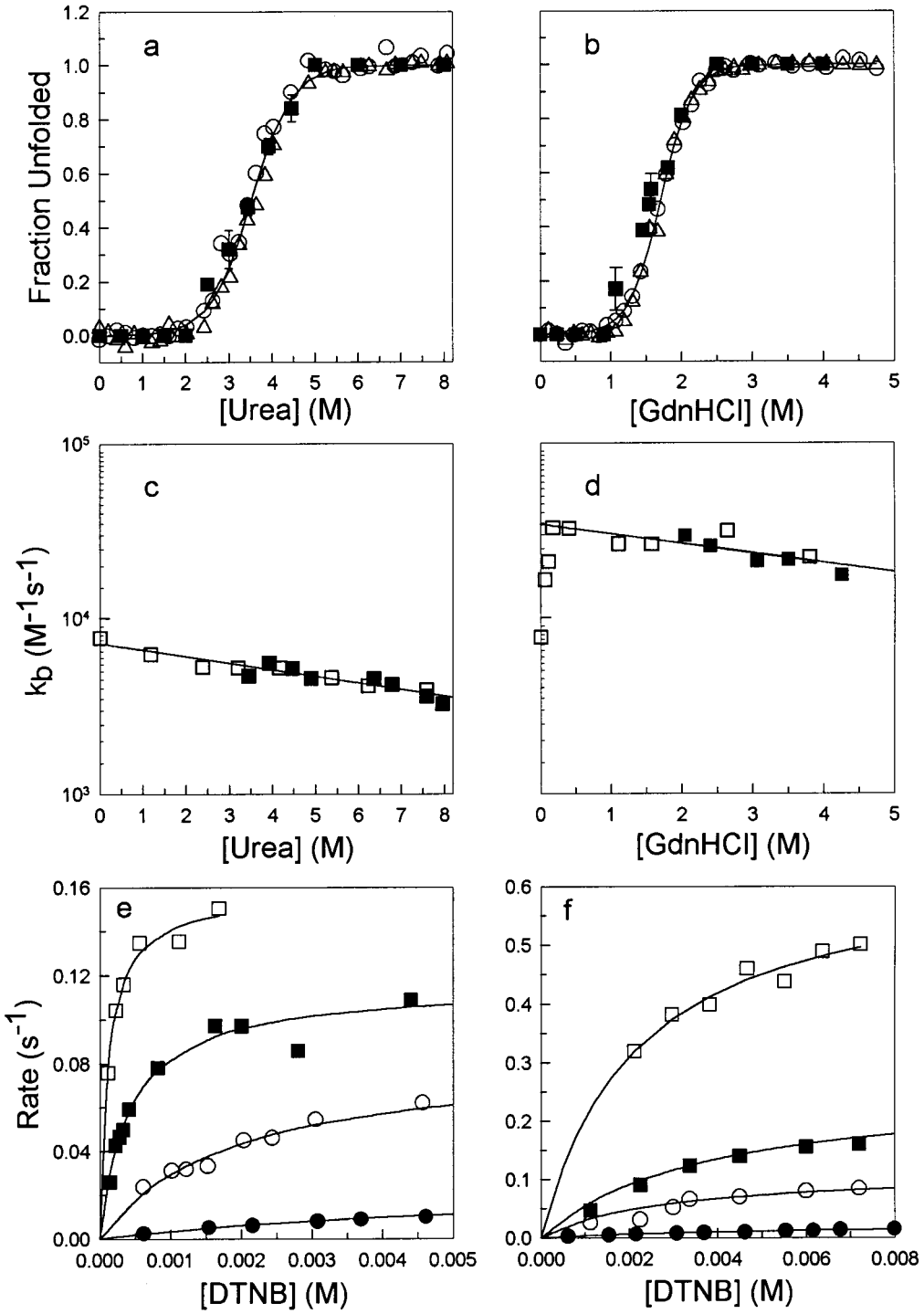


FIGURE 3: Amplitudes and rates of the fast and slow DTNB labeling reactions. (a and b) Equilibrium unfolding transition in urea (a) and GdnHCl (b) monitored by CD at 222 nm (open triangles) and tryptophan fluorescence at 320 nm (open circles). The fractional amplitude of the fast phase of the DTNB labeling of the protein equilibrated in different denaturant concentrations (closed squares). The error bars represent the standard error determined from multiple experiments. The solid lines through the data are obtained by fitting to a two-state, N ⇆ U equilibrium unfolding model. (c and d) The bimolecular rate constants ($k_b$) at different denaturant concentrations were obtained from the dependence of the fast labeling rate on DTNB concentration. Dependence of the bimolecular rate constant on urea (c) and GdnHCl (d) concentrations, determined by labeling the peptide (EGCDI) (open squares) or from the fast labeling rate obtained at high denaturant concentrations for barstar (closed squares). The lines represent linear regressions through the entire data in urea (c) and through the data from 0.2 to 5.0 M GdnHCl (d). (e and f) Dependence of the slow labeling rate observed with protein equilibrated in low denaturant concentrations at different DTNB concentrations: (e) in 0 (●), 2.1 (○), 3.2 (■), and 3.5 (□) M urea; (f) in 0 (●), 0.2 (○), 0.6 (■), 0.9 (□) M GdnHCl. The lines represent nonlinear least-squares fits to eq 4b.

greater than 0.2 M, and for urea, the bimolecular rate constant decreases with increasing denaturant concentration. This is probably because of the increase in viscosity of the reaction medium with increasing denaturant concentration. The denaturant dependence of the logarithm of $k_b$ was fit to a linear regression (Figure 3c,d), and the value of $k_b$ obtained from the fit at each denaturant concentration was used in the analysis of the slow labeling rates for the protein. The urea dependence of log $k_b$ was fit to a single linear regression, whereas the GdnHCl dependence of log $k_b$ from 0 to 0.2 M

and from 0.2 to 5.0 M was fit separately to different linear regressions.

The slow cysteine labeling rates observed in the pretransition and transition regions of denaturant concentration do not change linearly with DTNB concentration (Figure 3e,f). Within the transition region, the DTNB dependence of the slow labeling rates could be obtained only up to 4 M urea and up to 1.5 M GdnHCl. Beyond these denaturant concentrations in the transition regions, the rates showed negligible DTNB dependence even at very low DTNB concentrations, which is expected when $k_{cl}$ becomes slower than $k_{ex}$ at higher denaturant concentrations (see Discussion). Beyond the transition region, where only unfolded molecules are present at equilibrium, monitoring the kinetics of DTNB labeling only provides the labeling rate constant. The dependence of the slow labeling rate on DTNB at each denaturant concentration was fit to eq 4b. The bimolecular rate constant ($k_b$) obtained for the labeling of the peptide at different denaturant concentrations was used, and values for $k_{op}$ and $k_{cl}$ at each denaturant concentration were obtained from the fits.

Both the opening ($k_{op}$) and closing ($k_{cl}$) rate constants show a steep denaturant dependence (Figure 4a). $k_{cl}$ agrees, within experimental error, with the folding rate constant obtained by monitoring the fluorescence changes during the $U_F \rightarrow N$ transition. The most important observation from Figure 4a is that the $k_{op}$ obtained in low urea and GdnHCl concentrations converges to the rate obtained in the absence of denaturant (0.028 $s^{-1}$). Using the values of $k_{op}$ and $k_{cl}$ obtained by fitting the DTNB dependence of the labeling of the native protein, the free energy change calculated is $4.5 \pm 0.1$ kcal/mol, and this value agrees well with the value of $\Delta G_U(H_2O)$ obtained from the equilibrium unfolding transition.

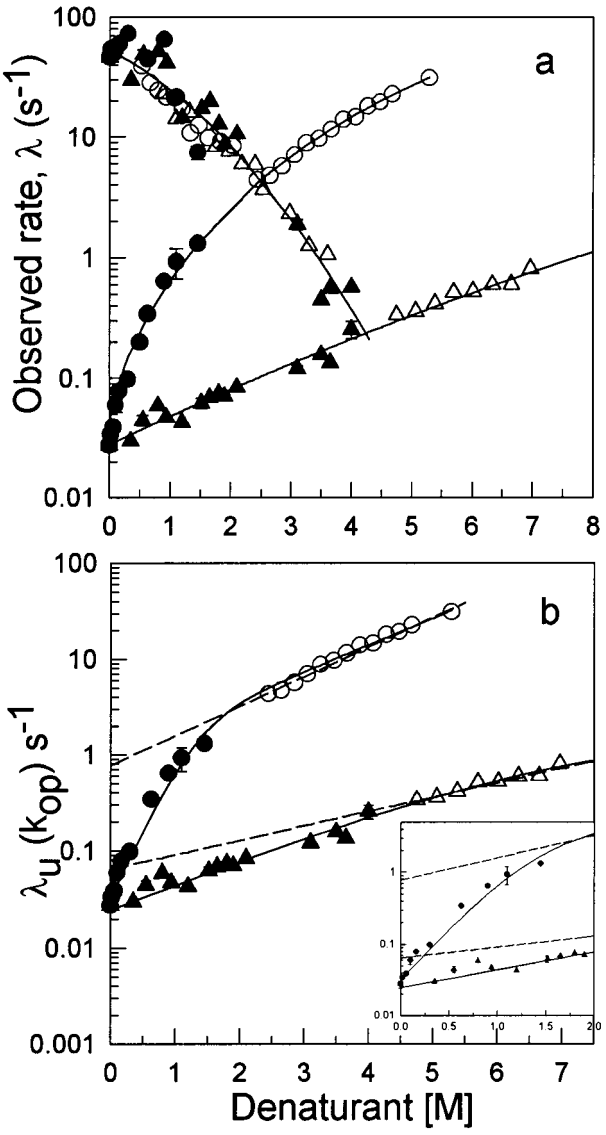


FIGURE 4: Observed folding and unfolding rates obtained by monitoring fluorescence changes and from the cysteine labeling method. Rates obtained by fluorescence-monitored kinetics are depicted as open symbols and rates obtained from cysteine labeling as closed symbols. (a) Rates in urea (triangles) and GdnHCl (circles). The line through the refolding rates represents $\log \lambda_f = -1.04 + 0.15[\text{denaturant}] + 0.04[\text{denaturant}]^2$, and the line through the unfolding data in urea represents $\log \lambda_u = -1.55 + 0.24[\text{urea}] - 0.004[\text{urea}]^2$. The line through the unfolding data in GdnHCl is drawn by inspection. (b) Unfolding rates in urea (triangles) and GdnHCl (circles). The dashed lines are fits to eqs 1a,b for the rates monitored by fluorescence (same as shown in Figure 1). The solid lines are fits to eq 7. The equilibrium constant ($K_1$) and the rate ($k_2$) obtained from the fits are $K_1 = (0.04)e^{0.49[\text{urea}]}$ and $k_2 = (0.6)e^{0.12[\text{urea}]}$ in urea and $K_1 = (0.03)e^{2.7[\text{GdnHCl}]}$ and $k_2 = (1.1)e^{0.64[\text{GdnHCl}]}$ in GdnHCl. The inset shows rates measured at the lowest concentrations of denaturants.

## DISCUSSION

*Determination of Unfolding Rates in Folding Conditions.* There have been only a few instances in the past where it has been possible to measure unfolding rates under native conditions. One strategy that was successful for the dimeric Arc repressor, where the unfolding reaction was coupled to dimer dissociation, was to use the change in efficiency of fluorescence resonance energy transfer between the monomers as they unfolded (*15*). Another strategy that was successful with the immunoglobulin light chain was to compare the rates of reduction of a buried disulfide bond with the unfolding rate (*40*). Here, it has been demonstrated that the thiol labeling reaction of a buried cysteine residue can be used for determining the global unfolding and refolding rates in zero or low denaturant concentrations. The strategy used should be generally applicable for any protein in which a single cysteine residue can be placed in a buried position by mutagenesis. A limitation of this method is that the cysteine introduced at a buried site should not alter the stability of the protein. It is certainly advantageous to use a naturally occurring buried cysteine residue, as done here in the case of barstar, where one of the two naturally occurring buried cysteine residues was mutated to alanine to get a single cysteine-containing protein.

It is important here to stress that the protein structure is very unlikely to be perturbed by the presence of the millimolar concentrations of DTNB used. Protein stability is not affected by the presence of DTNB: the fraction of protein unfolded at any denaturant concentration, as determined by the fraction of the labeling reaction that occurs fast, does not depend on the concentration of DTNB (0.5−8 mM) used. If the stability of the protein was indeed altered by DTNB, the fractional amplitude of the fast phase of labeling would not remain constant with a change in DTNB concentration.

*Similarities between Cysteine Labeling and Hydrogen Exchange.* The analysis of the observed labeling rate in the

cysteine labeling (SX) experiments reported here, based on mechanism 1 (eqs 4a,b; see Materials and Methods), was developed originally to provide a theoretical basis for amide hydrogen exchange (HX) reactions observed in proteins (*41*). The conformational openings that facilitate HX can be global unfolding, local unfolding, or limited native state fluctuations that do not involve appreciable unfolding (*32*, *42*). Labeling with the $TNB^-$ group is expected to perturb such structural events more than the introduction of hydrogen isotopes. The modified protein, which is as stable as the unmodified protein (*43*), does not, however, affect the rates in mechanism 1, and the observed SX and HX rates therefore reflect the same microscopic rate constants given in eqs 4a,b (*31*).

The dependence of the slow cysteine labeling rate on DTNB concentration was fit to eq 4b, with the assumption that the form reacting with DTNB has the thiol side chain as exposed as U and, hence, reacts with the same bimolecular rate constant ($k_b$). Determination of the opening rate constant $k_{op}$ is not influenced by the value of $k_b$: the opening event depends only on the stability of the closed state and is not influenced by the labeling reaction that follows. This is also evident from the form of eq 4b (*12*). The determination of the closing rate constant is, however, correlated with the value of $k_b$ because closing and labeling are competing reactions of the open state, and the relative magnitudes of these rates determine the fraction of molecules that get labeled. This was also verified by varying the value of $k_b$ in the fit: there was no effect on the value determined for $k_{op}$, but the value obtained for the closing rate $k_{cl}$ depended on the value used for $k_b$. Hence, an accurate value for $k_b$ at each denaturant concentration was independently determined by labeling a small pentapeptide flanking the sequence of Cys82 (Figure 3). It should be mentioned that, in the analysis of HX data also, the intrinsic HX rate in the protein is assumed to be the same as the intrinsic proton exchange rates observed in model peptides (*44*).

*Native State HX versus Native State SX*. Native state HX studies have yielded much valuable information about the structures of intermediates under native conditions and have also been used for determining the stability of the native state (*3*, *4*, *32*, *45*, *46*). Determination of folding and unfolding rate constants by use of the native state HX methodology depends on how fast the exchange reaction is compared to the folding (closing) reaction. When the intrinsic exchange rate ($k_{ex}$) is much faster than the closing rate constant ($k_{cl}$), then the observed rate ($k_{obs}$) is equal to the opening rate constant ($k_{op}$) (the EX1 limit). When $k_{ex}$ is much smaller than $k_{cl}$, then the observed rate is equal to $K_{op}k_{ex}$ (the EX2 limit), where $K_{op}$ ($=k_{op}/k_{cl}$) is the equilibrium constant for the formation of the exchange- (labeling-) competent state (see mechanism 1 and eq 4). Thus, to determine both $k_{op}$ and $k_{cl}$ from HX experiments, the exchange experiments have to be carried out over a wide range of conditions so that $k_{ex}$ varies sufficiently and, consequently, HX can be measured in the EX1 limit as well as in the EX2 limit. To vary $k_{ex}$ in HX experiments, it is necessary to vary pH over a wide pH range (~4−10), but this is not feasible for many proteins because usually protein stability varies considerably with change in pH. Thus, there are only a few instances of HX being used to determine $k_{op}$ and $k_{cl}$ (*11*, *23*). On the other hand, in the cysteine labeling methodology, variation of the exchange rate is achieved easily by changing the concentration of the labeling reagent, DTNB, without otherwise changing the conditions. Hence, it is relatively easy to determine $k_{op}$ and $k_{cl}$.

*Labeling of Cys82 Occurs in the Globally Unfolded State*. Several observations, evident in Figure 4, support the conclusion that the labeling-competent open form is the globally unfolded form and not an intermediate form: (i) both $k_{op}$ and $k_{cl}$ show steep denaturant dependences, unlike local unfolding events which show negligible denaturant dependence; (ii) the closing rate $k_{cl}$ agrees well with the refolding rates determined directly by observing the folding kinetics in either denaturant using tryptophan fluorescence; (iii) the value of $\Delta G_U(H_2O)$ obtained from the closing and opening rates in the absence of denaturant is comparable to the free energy change observed in the equilibrium unfolding transition monitored by CD or fluorescence; and (iv) the opening rates obtained in the presence of low concentrations of urea and GdnHCl converge to the same rate in the absence of denaturant. Thus, the apparent opening and closing rates correspond to the overall global unfolding and refolding rates, respectively.

*Unfolding in Native Conditions.* In the absence of any denaturant, native barstar has been shown to be capable of unfolding sufficiently so as to expose completely the buried cysteine side chain which can then react with DTNB. The rate at which this cysteine becomes exposed in the native state (0.028 $s^{-1}$) is similar to the rate of unfolding predicted from the directly observed refolding rate and the free energy change obtained from the equilibrium unfolding transition analyzed on the basis of a two-state model and the linear free energy extrapolation method. This implies that global unfolding similar to denaturant-induced unfolding occurs in native conditions, and it is likely that the native protein has sufficient conformational flexibility to sample a large number of partially folded states apart from the completely unfolded state.

Equilibrium amide HX studies of barstar have also shown that the free energy change for the formation of the exchange-competent state in low GdnHCl concentrations, determined from the rates of exchange of the slowest exchanging protons, is similar to the free energy change for the global unfolding transition monitored by optical probes (*3*). Thus, it is possible that the conformational space accessible to barstar is similar under native and denaturing conditions, and only the relative free energies of the different conformations change with denaturant.

*Nonlinear Denaturant Dependence of Log Rates.* The data in Figure 4a for the $N \rightarrow U_F$ reaction of barstar clearly show that the refolding rates when measured down to zero denaturant concentration show deviation from the linear equation (eq 2a). A similar curvature was seen for the logarithms of refolding rates monitored directly at low urea concentrations for *wt* barstar and was attributed to the presence of a folding intermediate in the folding pathway of $U_F$ to N (*24*). Nonlinearity in the logarithm of the unfolding rates is also evident for both denaturants (Figure 4b). The logarithm of the unfolding rates in urea varies smoothly with denaturant concentration whereas that of the unfolding rates in GdnHCl seems to vary in three distinct steps, each having a different denaturant concentration dependence (Figure 4b, inset). Such sharply kinked GdnHCl concentration dependence of log rates has previously been

observed for barnase, when the unfolding rates in low denaturant concentration were determined by folding and hydrogen exchange competition experiments (*23*), and the nonlinearity was attributed to the presence of on-pathway intermediates (*12*).

Deviations from the linear relationships of eqs 1a,b can also arise from the movement of the transition state during folding/unfolding with a change in denaturant concentration. According to the Hammond postulate (*47*), the closer the two states on a reaction pathway are in energy, the more their structures will resemble each other. If the exposure of the protein side chains is taken as the reaction coordinate, and greater exposure of buried groups results in higher energy states, then the position of the transition state will move toward the more unstable (exposed) state along the reaction coordinate. Since the stabilities of the native and unfolded proteins change with denaturant concentration, the position of the transition state is also expected to change with denaturant concentration, in accordance with the Hammond postulate. To account for Hammond behavior, the kinetic *m* values ($m_{\lambda_u}$ and $m_{\lambda_f}$) are usually assumed to have linear dependences on denaturant concentration (*16*, *48*). This results in the denaturant concentration dependence of the log rates according to eqs 1a,b to be quadratic instead of linear. In accordance with this, for proteins such as barnase and U1A, curved chevron plots have been fit to quadratic denaturant dependences (*16*, *48*). Despite the curvature in rates, the values for $\Delta G_U$ determined from the rates were found to be dependent linearly on denaturant concentration (eq 2) for U1A (*16*). This result was used as a justification for attributing the curvature to movement of the transition state and not due to the presence of any intermediates.

*Folding/Unfolding Kinetics of Barstar Are Not Two State*. The agreement of the value for $\Delta G_U(H_2O)$ obtained directly in the absence of denaturant from the cysteine labeling rates with the value obtained from the equilibrium unfolding transition, based on the linear free energy model, is expected either for a two-state reaction or for a multistate reaction in which the observed apparent rates obtained are defined by the rate constants of all the elementary reactions in the overall unfolding/refolding reaction. If the reaction in urea is, however, assumed to be two state and the curvature in the logarithm of the folding and unfolding rates is fit to quadratic expressions in denaturant concentrations (Figure 4a) to account for movements in the transition state, then the denaturant concentration dependence of $\Delta G_U$ determined from these rates is predicted to be nonlinear, because the curvature in the logarithm of the unfolding and refolding rates for barstar is not symmetric as in the case of U1A (*16*). The validity of the linear free energy relationship for barstar has, however, been established firmly in previous studies (*2*, *3*) and is further validated in this study by the agreement of the value of $\Delta G_U(H_2O)$ obtained by the cysteine labeling method with that obtained from the equilibrium unfolding transition. This implies that the quadratic equations used for describing the dependence of log rates with denaturant concentration are inappropriate for use in the case of barstar, and the nonlinearity observed in the denaturant dependence of the log rates indicates that the unfolding/folding of barstar cannot be two state.

The inappropriateness of a two-state model for describing the $N \rightleftharpoons U_F$ transition of barstar becomes more evident from the observation that the log of unfolding rates in GdnHCl cannot be described by a quadratic dependence on GdnHCl concentration, but, instead, a polynomial with higher order terms is required to describe the GdnHCl concentration dependence (Figure 4a). The logarithms of the unfolding rates in GdnHCl have an unusually steep dependence on GdnHCl concentration. This steep dependence on GdnHCl concentration compared to the much shallower dependence on urea concentration is unlikely to be the consequence of GdnHCl, but not urea, being an ionic denaturant. Barstar is stabilized in the presence of salts, and unfolding rates in high urea concentrations are reduced in the presence of 0.8 M KCl (*20*). The observed unfolding rates in low (<1 M) GdnHCl concentrations are, however, higher and not lower than the unfolding rates predicted on the basis of a two-state model from the free energy of unfolding, $\Delta G_U$, determined from the equilibrium unfolding transition and the observed folding rates. It should be noted that when the unfolding rates of ubiquitin were measured in low concentrations of GdnHCl by native state HX, they did not show a steeper dependence on GdnHCl concentration than that expected on the basis of a two-state unfolding model (*11*). The steeper dependence observed here for barstar therefore suggests non-two-state unfolding behavior.

In fact, the plot of log unfolding rate versus GdnHCl concentration appears to have two sharp inflections, at 0.3 M GdnHCl and at 1.5 M GdnHCl (Figure 4b, inset). Sharp inflections in plots of rate constants are inconsistent with a smooth movement of the transition state (*12*, *15*) and are usually due to a change in the rate-determining step or a change of mechanism. The presence of parallel pathways that differ in the degree of exposure of the transition state can also lead to such kinks (*12*), and when each pathway has essentially the same activation energy barrier (see below), the kink need not be upward (*21*). It is therefore clear that the curvatures in both arms of the chevron plots of barstar, seen for urea as well as GdnHCl, cannot be described adequately by movements in the transition state during folding/unfolding, and the curvatures are more likely to be the consequence of the folding/unfolding reaction being more complex than a simple two-state reaction.

Indirect support for the existence of parallel pathways is also provided by the observation that refolding rates in urea and GdnHCl (Figure 4a) are identical at identical molar concentrations. The coincidence of refolding rates in urea and GdnHCl indicates that the activation energy barrier for refolding is the same in either denaturant. Information about the solvent exposure of the transition state during refolding can be obtained from the denaturant concentration dependence of the logarithm of the refolding rates ($m_{\lambda_f}$) and of the free energy change during equilibrium unfolding ($m_G$). The *m* value for any transition represents the difference in the extent of solvent exposure between the two states involved in the transition. The extent of solvent exposure of the transition state during folding can be estimated from the Tanford $\beta$ value ($\beta_T$), which is defined as the ratio of the dependence on the denaturant concentration of the free energy of activation for folding ($\Delta G_{\ddagger-D}$) and of the equilibrium free energy of unfolding ($\Delta G_U$) (*14*). Although the denaturant concentration dependence of the free energy of activation for folding is the same in either denaturant (because the folding rates are identical), the value of $m_G$ is

2-fold higher in GdnHCl than in urea. The $\beta_T$ values for the folding transition state are therefore different in urea and GdnHCl. The simplest explanation for this would be that different pathways are utilized in urea and in GdnHCl, because it is unlikely that energetically similar but structurally dissimilar transition states occur on the same pathway. Earlier kinetic experiments have shown that intermediates accumulate during the $N \rightarrow U_F$ unfolding transition of barstar at high denaturant concentrations (*20*, *29*, *49*, *50*). The nonlinear dependence of the logarithms of the folding and unfolding rates seen here at low denaturant concentrations indicate the existence of intermediates at low denaturant concentrations also.

*A Three-State Unfolding Pathway.* A minimal three-state model (mechanism 2), where intermediate I has a buried cysteine residue like the native protein and labeling occurs only from the globally unfolded U state, was used to analyze the observed folding and unfolding rates in urea and GdnHCl. It is evident that an intermediate with an exposed cysteine residue cannot form rapidly because the entire labeling kinetics would then be very fast, unlike the slow labeling rates observed here. In this model, if a fast preequilibrium (determined by the equilibrium constant $K_1$) is established between N and I, and I unfolds to U, the observed unfolding and folding rates are given by eqs 7 and 8. When fit to eq 7, the observed unfolding rates yield values for $K_1$ and the rate $k_2$, as well as their dependences on denaturant concentration (see legend to Figure 4). The logarithm of all the rate constants is assumed to vary linearly with denaturant concentration. The value obtained for the equilibrium constant $K_1$ (see legend to Figure 4) indicates that, in the absence of denaturant, I is populated only to the extent of 3−4%. It would have been unlikely for this small fraction of I to have been detected by any of the optical probes or by NMR spectroscopy that has been used in the past for studying the folding/unfolding reactions of barstar (*3*, *25*−*27*). The free energies of I and U relative to that of the native state were determined from $K_1$, and the global free energy change was determined from the equilibrium unfolding transition (Figure 5).

It has not been the purpose of this study to determine a detailed multistate mechanism for the unfolding of barstar at low denaturant concentrations. The purpose has been more to demonstrate that the mechanism is not a simple two-state one. It is clear that mechanism 2, with the assumption of a fast preequilibrium between N and I, is the simplest scheme that describes the observed data somewhat reasonably, but close inspection of the data in Figure 4b (see inset) shows that it is clearly not completely adequate: the fit of the data in Figure 4b to the equation derived from mechanism 2 is clearly not good at very low GdnHCl concentrations. When the data were simulated to more complex mechanisms with two intermediates either appearing sequentially on one pathway or on parallel pathways, better fits could be obtained. The improvements to the fits that were seen were however judged not to be good enough to warrant the invocation of the more complex mechanisms at this stage. The inadequacy of mechanism 2 is also reflected in the observation that the fits to eq 7 did not yield unique values for $K_1$ and $k_2$ nor for their dependences on denaturant concentration. The values which agreed best with the global free energy change and its denaturant dependence have been reported.

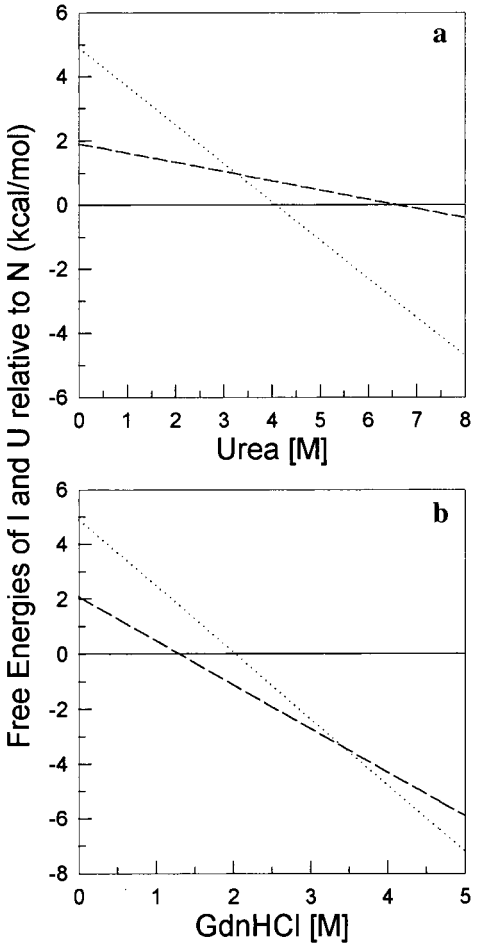


FIGURE 5: Denaturant concentration dependence of the free energies of I and U relative to that of N. Free energies were determined from the values of $K_1$ and $K_U$ at each denaturant concentration, according to mechanism 2. The solid line represents the N state, the dashed line represents the I state, and the dotted line corresponds to the U form, in urea (a) and GdnHCl (b).

*Conclusions.* It has been shown that measurement of the accessibility of a buried cysteine residue in a protein by use of a simple thiol labeling reaction is a valid approach to study the mechanism of protein folding and unfolding. Monitoring the rates of DTNB labeling reactions allows the global unfolding and refolding rates to be determined. The method demonstrates that linear extrapolation of the logarithm of rates may not always be reliable. In particular, determination of unfolding rates of barstar in the absence of any denaturant and in low concentrations of denaturant shows that the denaturant dependence of logarithm of rates is nonlinear due to non-two-state folding behavior.

## ACKNOWLEDGMENT

We thank members of our laboratory for discussion.

## REFERENCES

1. Schellman, J. A. (1987) *Annu. Rev. Biophys. Chem. 16*, 115−137.
2. Agashe, V. R., and Udgaonkar, J. B. (1995) *Biochemistry 34*, 3286−3299.
3. Bhuyan, A. K., and Udgaonkar, J. B. (1998) *Proteins: Struct., Funct., Genet. 30*, 295−308.
4. Huyghues-Despointes, B. M. P., Scholtz, J. M., and Pace, C. N. (1999) *Nat. Struct. Biol. 6*, 910−912.

5. Englander, S. W. (2000) *Annu. Rev. Biophys. Biomol. Struct. 29*, 213−238.
6. Jackson, S. E., and Fersht, A. R. (1991) *Biochemistry 30*, 10428−10435.
7. Guijarro, J. I., Morton, C. J., Plaxco, K. W., Campbell, I. D., and Dobson, C. M. (1998) *J. Mol. Biol. 276*, 657−667.
8. Plaxco, K. W., Guijarro, J. I., Morton, C. J., Pitkeathly, M., Campbell, I. D., and Dobson C. M. (1998) *Biochemistry 37*, 2529−2537.
9. Wittung-Stafshede, P., Lee, J. C., Winkler, J. R., and Gray, H. B. (1999) *Proc. Natl. Acad. Sci. U.S.A. 96*, 6587−6590.
10. Plaxco, K. W., Simons, K. T., Ruczinski, I., and Baker, D. (2000) *Biochemistry 39*, 11177−11183.
11. Sivaraman, T., Arrington, C. B., and Robertson, A. D. (2001) *Nat. Struct. Biol. 8*, 331−333.
12. Fersht, A. R. (2000) *Proc. Natl. Acad. Sci. U.S.A. 97*, 14121−14126.
13. Matouschek, A., Kellis, J. T., Jr., Serrano, L., Bycroft, M., and Fersht, A. R. (1990) *Nature 346*, 440−445.
14. Matouschek, A., and Fersht, A. R. (1993) *Proc. Natl. Acad. Sci. U.S.A. 90*, 7814−7818.
15. Jonsson, T., Waldburger, C. D., and Sauer, R. T. (1996) *Biochemistry 35*, 4795−4802.
16. Otzen, D. E., Kristensn, O., Proctor, M., and Oliveberg, M. (1999) *Biochemistry 38*, 6499−6511.
17. Dalby, P. A., Oliveberg, M., and Fersht, A. R. (1998) *J. Mol. Biol. 276*, 625−646.
18. Llinás, M., Gillespie, B., Dahlquist, F. W., and Marqusee, S. (1999) *Nat. Struct. Biol. 6*, 1072−1078.
19. Parker, M. J., and Marqusee, S. (1999) *J. Mol. Biol. 293*, 1195−1210.
20. Zaidi, F. N., Nath, U., and Udgaonkar, J. B. (1997) *Nat. Struct. Biol. 4*, 1016−1024.
21. Bachmann, A., and Kiefhaber, T. (2001) *J. Mol. Biol. 306*, 375−386.
22. Matouschek, A., Otzen, D. E., Itzhaki, L. S., Jackson, S. E., and Fersht, A. R. (1995) *Biochemistry 34*, 13656−13662.
23. Takei, J., Chu, R. A., and Bai, Y. (2000) *Proc. Natl. Acad. Sci. U.S.A. 97*, 10796−10801.
24. Schreiber, G., and Fersht, A. R. (1993) *Biochemistry 32*, 11195−11203.
25. Shastry, M. C., Agashe, V. R., and Udgaonkar, J. B. (1994) *Protein Sci. 3*, 1409−1417.
26. Shastry, M. C., and Udgaonkar, J. B. (1995) *J. Mol. Biol. 247*, 1013−1027.
27. Agashe, V. R., Shastry, M. C., and Udgaonkar, J. B. (1995) *Nature 377*, 754−757.
28. Nath, U., Agashe, V. R., and Udgaonkar, J. B. (1996) *Nat. Struct. Biol. 3*, 920−923.
29. Ramachandran, S., Rami, B. R., and Udgaonkar, J. B. (2000) *J. Mol. Biol. 297*, 733−745.
30. Sridevi, K., Juneja, J., Bhuyan, A. K., Krishnamoorthy, G., and Udgaonkar, J. B. (2000) *J. Mol. Biol. 302*, 479−495.
31. Ha, J.-H., and Loh, S. N. (1998) *Nat. Struct. Biol. 5*, 730−737.
32. Bai, Y., Sosnick, T. R., Mayne, L., and Englander, S. W. (1995) *Science 269*, 192−197.
33. Khurana, R., Hate, A. T., Nath, U., and Udgaonkar, J. B. (1995) *Protein Sci. 4*, 1133−1144.
34. Paul, C., Kirschner, K., and Haenisch, G. (1980) *Anal. Biochem. 101*, 442−448.
35. Jocelyn, P. C. (1987) *Methods Enzymol. 143*, 44−67.
36. Snyder, G. H., Cennerazzo, M. J., Karalis, A. J., and Field, D. (1981) *Biochemistry 20*, 6509−6518.
37. Santoro, M. M., and Bolen, D. W. (1988) *Biochemistry 27*, 8063−8068.
38. Cleland, W. W. (1975) *Biochemistry 14*, 3220−3224.
39. Fersht, A. R. (1999) in *Structure and Mechanism in Protein Science*, pp 122−125, W. H. Freeman and Co., New York.
40. Kikuchi, H., Goto, Y., and Hamaguchi, K. (1986) *Biochemistry 25*, 2009−2013.
41. Hvidt, A., and Nielsen, S. O. (1966) *Adv. Protein Chem. 21*, 287−386.
42. Kim, K. S., Fuchs, J. A., and Woodward, C. K. (1993) *Biochemistry 32*, 9600−9608.
43. Lakshmikanth, G. S., Sridevi, K., Krishnamoorthy, G., and Udgaonkar, J. B. (2001) *Nat. Struct. Biol. 8*, 799−804.
44. Bai, Y., Milne, J. S., Mayne, L., and Englander, S. W. (1993) *Proteins 17*, 75−86.
45. Chamberlain, A. K., Handel, T. M., and Marqusee, S. (1996) *Nat. Struct. Biol. 3*, 782−787.
46. Parker, M. J., and Marqusee, S. (2001) *J. Mol. Biol. 305*, 593−602.
47. Hammond, G. S. (1955) *J. Am. Chem. Soc. 77*, 334−338.
48. Johnson, C. M., and Fersht, A. R. (1995) *Biochemistry 34*, 6795−6804.
49. Rami, B. R., and Udgaonkar, J. B. (2001) *Biochemistry 40*, 15267−15279.
50. Nath, U., and Udgaonkar, J. B. (1995) *Biochemistry 34*, 1702−1713.

BI011494V